Winter-to-Winter Recurrence of Sea Surface Temperature, Salinity and Mixed Layer Depth Anomalies

Michael A. Alexander*
Mike S. Timlin
James D. Scott

NOAA-CIRES/Climate Diagnostics Center
University of Colorado
(Submitted to Progress in Oceanography
Special Issue: Beyond El Niño Conference)
March 2000

*Corresponding author address:
Dr. Michael Alexander
NOAA-CIRES/Climate Diagnostics Center
R/E/CDC1
325 Broadway
Boulder, CO 80303-3328
email: maa@cdc.noaa.gov

ABSTRACT

The mean seasonal cycle of mixed layer depth (MLD) in the extratropical oceans has the potential to influence temperature, salinity and mixed layer depth anomalies from one winter to the next. Temperature and salinity anomalies that form at the surface and spread throughout the deep winter mixed layer are sequestered beneath the mixed layer when it shoals in spring and are then re-entrained into the surface layer in the subsequent fall and winter. Here we document this “reemergence mechanism” in the North Pacific Ocean using observed SSTs, subsurface temperature fields from a data assimilation system, and coupled atmosphere-ocean model simulations. Observations indicate that the dominant large-scale SST anomaly pattern that forms in the North Pacific during winter recurs in the following winter. The model simulation with mixed layer ocean physics reproduced the winter-to-winter recurrence, while model simulations with observed SSTs specified in the tropical Pacific and a 50 m slab in the North Pacific did not. This difference between the model results indicate that the winter-to-winter SST correlations are due to the reemergence mechanism and not by similar atmospheric forcing of the ocean in consecutive winters and that SST anomalies in the tropical Pacific associated with El Niño are not essential for reemergence to occur.

The recurrence of observed SST and simulated SST and SSS anomalies are found in several regions in the central North Pacific and are quite strong in the northern (> 50°N) part of the basin. The winter-to-winter autocorrelation of SSS anomalies exceed those of SST, since only the latter are strongly damped by surface fluxes. The reemergence mechanism also has a modest influence on MLD through changes in the vertical stratification in the seasonal thermocline.

1. Introduction

El Niño and the Southern Oscillation (ENSO), a coupled atmosphere-ocean phenomena in the equatorial Pacific that varies over a period of about 2-7 years, has a significant impact on climate variability and ecosystems over the globe. During strong El Niño events, drastic changes occur in the eastern tropical Pacific Ocean: rainfall is greatly enhanced, sea surface temperatures (SSTs) warm by more than 3°C, the normal upwelling of cold nutrient rich water ceases and populations of many marine species decline precipitously (Barber and Chavez, 1983, Philander, 1990; Glynn, 1990). ENSO also influences conditions over the North Pacific: coastal Kelvin waves act to warm the water within a ~100 km of the North American coast (Enfield and Allen, 1980; Pares-Sierra and O'brien, 1989; Meyers et al., 1996), while changes in the atmospheric circulation cools the central Pacific Ocean and warms the eastern third of the basin via changes in air-sea heat fluxes (Alexander, 1992; Lau and Nath, 1996). ENSO induced changes in currents, temperatures, etc. over the North Pacific appears to have influenced fish populations, including the migration routes of salmon and tuna (Mysak, 1986) and the abundance of rockfish (Yoklavich et al., 1996).

Several other processes also affect climate variability in the North Pacific on time scales of both longer and shorter duration than ENSO. A number observational studies have documented decadal (> ~10 years) variability in the North Pacific (Tanimoto, 1993; Trenberth and Hurrel, 1994; Mantua et al., 1997; Nakamura et al., 1997). Several studies have proposed, that like ENSO, it is conditions in the tropical Pacific that are governing this lower frequency variability (Graham et al., 1994; Trenberth and Hurrell, 1994), while others indicate air-sea interaction and ocean dynamics in midlatitudes are the key source of this variability (Latif and Barnett, 1994; 1996; Jin, 1997; Talley, 1999).

Widespread ecological fluctuations on decadal time scales have also been noted. Many studies have focused on ecosystem changes associated with an abrupt cooling in the central North Pacific that began in 1976 and lasted until 1988. Venrick et al. (1987) found that chlorphyll in the water column, a measure of primary productivity, increased during this period, while Brodeur and Ware (1992) and Roemmich and McGowan (1995) noted changes in zooplankton levels. Ebbesmeyer et al. (1991) documented an abrupt transition in many land and marine species around 1976, and several studies, including (McFarlane and Beamish, 1982; Polovina et al., 1994) have found evidence for changes in fish stocks around this time. Taken together these studies suggest that the climate fluctuations change phytoplankton productivity, which in turn affect higher trophic levels. Results from Beamish and Boullion (1993), Francis and Hare (1994), and Mantua et al. (1997) indicate that the regime change in the 1970's is not unique in the climate record but one of several interdecadal climate fluctuations that occurred in the 20th century.

On annual and shorter time scales variability in the large-scale patterns of extratropical SST anomalies has mainly been attributed to local processes, including air-sea heat fluxes and vertical mixing in the upper ocean (Gill and Niiler 1972; Frankignoul and Reynolds 1983; Frankignoul 1985; Delworth, 1996). The surface layer of most of the world's oceans is vertically well mixed with nearly uniform temperature and salinity. In response to the seasonal cycle in wind stirring and surface buoyancy forcing, the ocean mixed layer deepens through fall and winter due to entrainment and then reforms close to the surface in spring and remains shallow through late summer. In the North Pacific the mean mixed layer depth (MLD) ranges from ~20 m in summer to more than 100 m in winter, while departures in MLD from the seasonal mean can significantly influence SSTs (Elsberry and Garwood, 1978; Alexander et al., 2000).

Mixed layer depth is a crucial factor in phytoplankton production since entrainment of deeper water into the mixed layer increases the supply of nutrients but also mixes phytoplankton deeper where less light is available for photosynthesis (Cullen and Lewis, 1988; Mann and Lazier, 1991; Denman and Gargett, 1995). Several studies, including Marra and Ho (1993), Sarmiento et al. (1993), Fashom (1995), and Doney et al. (1996) have examined the relationship between upper ocean mixing and biological productivity over the course of the seasonal cycle using coupled biological-physical models. Polovina et al. (1995) found that atmospheric forcing over the North Pacific lead to decadal variations in MLD, which in turn, strongly influenced biological productivity.

The seasonal cycle of MLD has the potential to influence conditions in the upper ocean from one winter to the next. Namias and Born (1970, 1974) were the first to note a tendency for midlatitude SST anomalies to recur from one winter to the next without persisting through the intervening summer. They speculated that temperature anomalies that form at the surface and spread throughout the deep winter mixed layer remain beneath the mixed layer when it shoals in spring. The thermal anomalies are then incorporated into the stable summer seasonal thermocline (30-100 m) where they are insulated from surface fluxes. When the mixed layer deepens again in the following fall, the anomalies are re-entrained into the surface layer and influence the SST. Using subsurface temperature data from ocean weather ships and one-dimensional mixed layer model simulations Alexander and Deser (1995) found that this "reemergence mechanism" (shown schematically in Fig. 1) occurred at several locations remote from strong ocean currents. Bhatt et al. (1997) and Watanabe and Kimoto (2000) found further evidence for the reemergence of SST anomalies in the North Atlantic Ocean. Alexander et al. (1999) used several ocean temperature datasets to show that the reemergence mechanism occurred across much of the North Pacific Ocean, where the dominant SST anomaly pattern that forms during late winter, returns in the following fall/winter, with little persistence at the surface in summer.

In the present study, we expand on the work of Alexander et al. (1999) by addressing the following questions: Can we simulate the reemergence process in the North Pacific using a coupled atmosphere-ocean model? The reemergence mechanism has not been well documented in the far North Pacific; is it strong in this region where winter MLDs are relatively deep? Could SST anomalies reappear in the North Pacific from one winter to the next as a result of atmospheric forcing, such as consecutive winters of a stronger than normal Aleutian low, rather than by the reemergence mechanism? Is ENSO critical for the winter-to-winter recurrence of SST anomalies over the North Pacific? Does reemergence influence fields other than temperature that also have the potential to influence marine ecosystems, such as salinity and mixed layer depth?

2. Observations and Model Simulations

In the present study we use SST data, temperature analyses from an ocean data assimilation system, and coupled atmosphere-ocean model simulations to examine the reemergence mechanism over the North Pacific. The gridded SST data, from Smith et al. (1996), uses a statistical method to fills data voids and create fields that emphasize large-scale features. Global monthly SST fields are available from the Smith analyses on a 2°x2° grid for 1950-1992. From 1993-2000 we use the SSTs on a 1°x1°grid based on the Reynolds and Smith (1994) optimal interpolation scheme.

Currently, there are not enough upper ocean temperatures measurements necessary for documenting the reemergence mechanism across the North Pacific. Here,

Re-emergence Mechanism Schematic

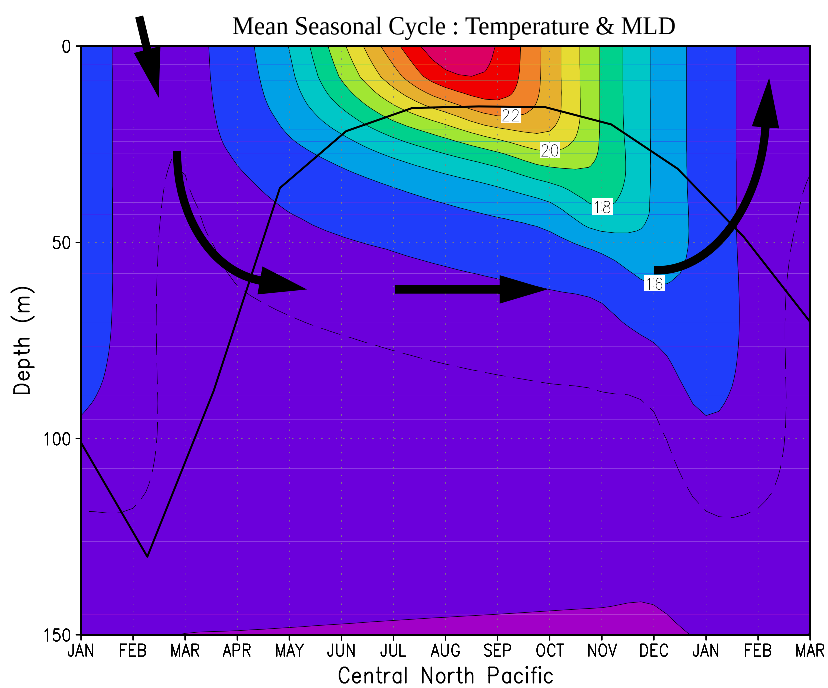

.Fig. 1. Mean seasonal cycle of upper ocean temperature (˚C) and mixed layer depth (m) for the central North Pacific (28˚-42˚N, 180˚-165˚E) from the AGCM-MLM simulation. The arrows indicate the path of the reemergence mechanism where anomalies created in winter are stored in the summer seasonal thermocline and are re-entrained into mixed layer when it deepens in the following fall and winter. Conour interval is 1ºC.

we use monthly temperature fields obtained from the ocean data assimilation system at the National Center for Environmental Prediction (NCEP). The NCEP ocean data assimilation system, described by Derber and Rosati (1989) and Ji et al. (1995), consists of observations of SST taken from satellites and ships, plus subsurface thermal profiles obtained from expendable bathythermographs, that are blended with fields from an ocean general circulation model. The system domain is between 35°S and 45°N in the Pacific; the upper ocean is well resolved with 10 (15) levels in the upper 100 (200) m. We assume that the temperature obtained from the top level (5 m) is representative of the SST. We use monthly mean temperatures from the assimilation system from its start in January of 1980 through June of 1998.

Most of the model results presented here are derived from a 50-year simulation of a global coupled atmosphere-ocean model. The model, described in detail by Alexander et al. (2000), consists of the Geophysical Fluid Dynamics Lab (GFDL) atmospheric general circulation model (AGCM) connected to an upper ocean mixed layer model (MLM). By using a coupled model we avoid the very difficult task of finding appropriate boundary conditions for the ocean model. The MLM, which is comprised of a grid of independent column models that are aligned with AGCM grid, simulates SST, sea surface salinity, and mixed layer depth (MLD). The MLM is based on the formulation of Gaspar (1988); and includes local atmosphere-ocean fluxes and the turbulent entrainment of water into the surface mixed layer, but not mean vertical motions or horizontal processes. The region beneath the mixed layer is represented by a multi-layer system where heat is redistributed via convective overturning, vertical diffusion, and penetrating solar radiation. By design, the AGCM-MLM simulation enables us to study the affects of midlatitude air-sea interaction and mixed layer physics, since it does not include western boundary currents or ENSO.

We will also examine a second set of model experiments in which the GFDL AGCM has observed SSTs prescribed as boundary conditions in the tropical Pacific Ocean between approximately 25°N-25°S for the years 1950-1995. Outside of this domain the AGCM is coupled to a 50 m slab model over the remainder of the global ocean, where SSTs are regulated solely by the net surface heat flux. There is a set of four of these simulations that differ only in their initial atmospheric states. In keeping with previous naming conventions, these simulations are referred to as the “tropical ocean global atmosphere” – 50 m slab ocean (TOGA-50m) experiment. Due to errors in the atmospheric fluxes and the absence of ocean heat transport, a surface heat flux correction is applied in both the TOGA-50m and the AGCM-MLM experiments, in order to maintain a reasonable SST climatology.

All of the fields from both model and observations have been interpolated onto a 4ºx4º grid over the North Pacific. The analyses have been performed using monthly anomalies, defined as the departure of the mean value for a given month from the long-term monthly mean.

3. Results

a. regional analyses

The mean seasonal cycle of temperature and mixed layer depth from the 50-year AGCM-MLM simulation are shown for a region in the central North Pacific in Fig. 1. The MLD reaches a maximum of ~135 m in February and shoals rapidly in spring, reaching a minimum depth of ~20 m from June through September. A seasonal thermocline, where the temperature decreases rapidly with depth, forms in the summer between the base of the mixed layer and ~80 m. While the model simulates the key aspects of the seasonal cycle necessary for reproducing the reemergence mechanism, there are some differences with observations (not shown): the simulated MLD is ~10% too shallow in fall and winter and, as a result, the fall temperature maximum does not penetrate as deep in the MLM.

We examine the reemergence mechanism in regions where previous analyses suggest that it is strong: along the North American coast in the east Pacific, north of Hawaii in the central Pacific and along 40°N in the west Pacific. Regressions between SST anomalies in February-March-April (FMA) with temperature anomalies as a function of depth and month are shown for observations, provided by the NCEP data assimilation system, and the MLM in Fig. 2. The regression analyses provides a linear estimate of how an SST anomaly of 1°C in spring evolves from the previous January through the following April, allowing one to track the magnitude of an anomaly through the full reemergence process. A 1°C anomaly is fairly large, as the standard deviation of SST is about $1/2 - 3/4$ °C in late winter. The regressions indicate the reemergence mechanism occurs in all three regions in both the model and observations: high regression values that extend over the deep winter mixed layer, are maintained in and below the seasonal thermocline but decay at the surface in summer, and then increase again at the surface in the following fall-winter.

Several factors influence the timing and strength of the reemergence mechanism including variations in the mean seasonal cycle of mixed layer depth. The maximum MLD in the North Pacific increases from about 80 m along the west coast of North America, to 120 m in

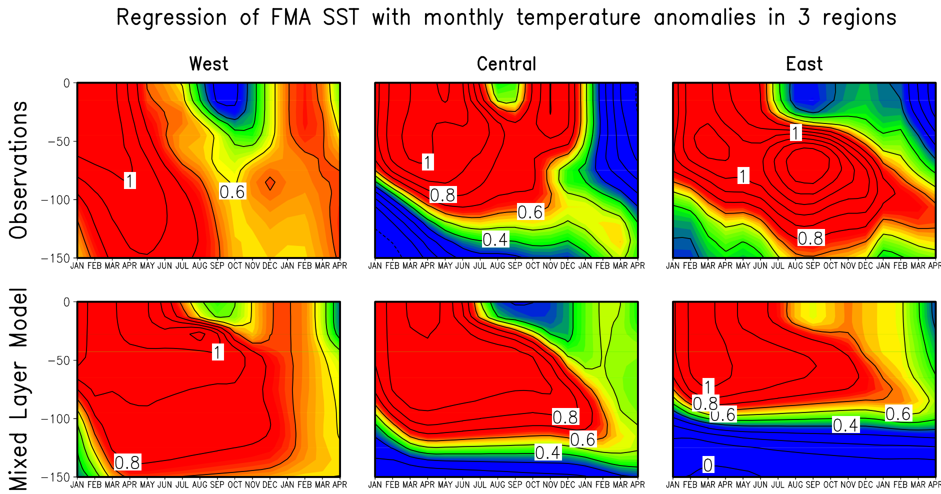

Fig. 2. Lead-lag regressions (˚C per 1˚C) between SST anomalies in February-March-April (FMA) and temperature anomalies from the previous January through the following April in the eastern (26N˚-42˚N, 132˚W-116˚W), central (26N˚-42˚N, 164˚W-148˚W), and western (38˚N-42˚N, 160˚E-180˚) regions. Values are computed from observations provided by the NCEP ocean assimilation system for the years 1980-1998 and from the 50-year AGCM-MLM simulation. Contour interval is 0.1 ˚C per 1˚C.

the central Pacific, and 200 m east of Japan (Bathen, 1972; Deser et al., 1996; Alexander et al., 2000). As a result, the depth to which temperature anomalies penetrate in late winter increases from east to west, especially in the MLM as suggested by Fig 2. The vertical extent of temperature anomalies below the mixed layer is influenced by the stability of the seasonal thermocline and its interaction with the deeper ocean. In observations, the temperature anomalies created in winter continue to propagate down with time, due to subduction and complex turbulent processes, while in the MLM, without these processes, temperature anomalies remain at nearly the same depth through summer and fall. Several other factors could also lead to differences between the MLM and observations in the structure of the reemergence mechanism, including: the short duration of the observed time series, errors in the atmospheric surface forcing and in the mixed layer physics, and the absence of currents in the MLM.

The relatively deep winter mixed layers (> 150 m) in the far North Pacific in both the MLM and observations suggest that the winter-to-winter persistence of SSTs could be strong there. Alexander and Deser (1995) found evidence for the reemergence mechanism at weather ship P (50°N, 145°W), however the NCEP ocean assimilation only extends to 45º Nand most broad scale examinations of this process were performed farther to the south. Here we show correlations at 52°N between SST anomalies in FMA with monthly SST anomalies from the previous January through the following June. These autocorrelations are shown in Fig. 3 for both the Smith et al. (1996) SST data set and from the MLM in each grid square between 160°E and 130°W. Across the basin in both observations and the model, high correlations in winter (>0.7) decrease through spring reaching a minimum in summer (0.1-0.4) and then increase through fall and reach a maximum (>0.5) in the following winter. While the observed and simulated values are not identical, both indicate that the summer mimima last longer and are stronger in the eastern and western portions of the basin relative to the central Pacific and the return to higher correlations occurs earlier in the central (160°W) than in the west (165°E) Pacific.

b. Basin-wide analyses

The behavior of thermal anomalies across the North Pacific over the seasonal cycle is examined using extended empirical orthogonal function analysis (EEOFs). EOF analysis is a method for finding patterns in a field of variables. EEOFs indicate how patterns evolve with time, and have been used in several studies to examine the evolution of climate anomalies (e.g. Weare and Nastrom, 1982; Lau et al., 1992; Miller et al., 1998). Here, the leading EEOF of monthly SST anomalies from January through the following April (lags of 0-15 months) is computed from the covariance matrix, where the variance at each point in a month has been normalized by the average standard deviation of SST at all points in the domain during that month. EEOF 1 is presented as the correlations between the first principal component (i.e. the time series that gives the sign and amplitude of EEOF 1 in each year) and the time series

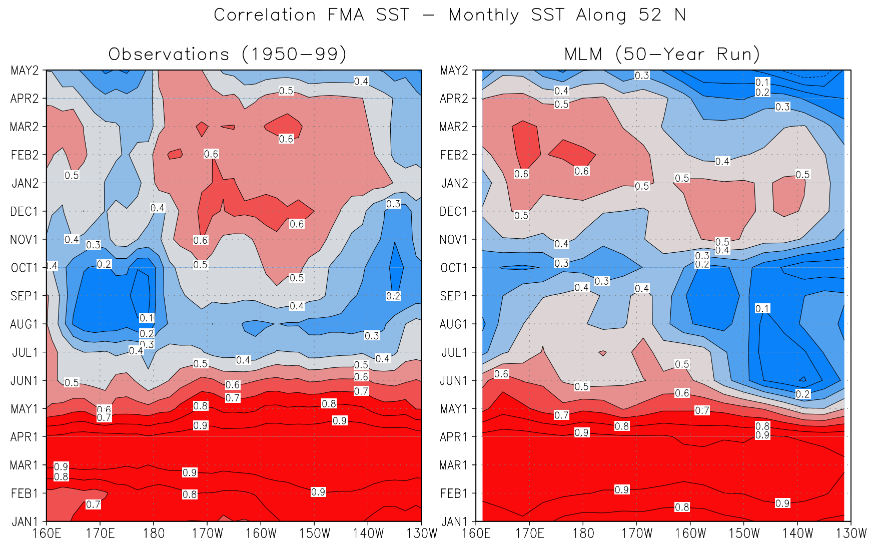

Fig. 3: Lead-lag correlations between SST anomalies in FMA and monthly SST anomalies from the previous January through the following May for each grid box along 52˚N from (a) observations and (b) the MLM. Contour interval is 0.1.

of monthly SST anomalies at individual grid points.

The evolution of the leading pattern of SST variability and the percent variance explained by EEOF 1 in each month from January through the following April are shown in Fig. 4 for (a) observations, (b) the AGCM-MLM and (c) the set of four TOGA-50m simulations. Recall that the same AGCM is used in both simulations, but in the latter SSTs are specified according to observations over the period 1950-1995 in the tropical Pacific, while SSTs are simulated by a 50 m slab model elsewhere over the global ocean. Thus, the TOGA-50m experiments do have the ENSO signal in the tropical Pacific but do not have mixed layer physics in the North Pacific. EEOF 1 explains approximately the same amount of total variance (15%-18%) in observations and the two model simulations. The leading pattern of variabilty in the three analyses are also similar: all show anomalies of one sign from about 25°N-45°N in the central and west Pacific ringed by anomalies of the opposite sign. In observations and the MLM the magnitude of the pattern and the percent variance explained decreases from March to a minumum in September and then increases again reaching a maximum in the following winter. However, in the TOGA-50m simulations the magnitude decreases with time and the pattern nearly disappears by November. The capacity of the AGCM-MLM to simulate the evolution of the dominant pattern of SST variability over the North Pacificwhile the the TOGA-50m did not has several important implications: i) the winter-to-winter recurrence of SST anomalies is not due to similar atmospheric forcing patterns from one winter to the next; ii) ENSO events are not crucial for getting the winter-to-winter basin-wide SST anomaly pattern; and iii) the MLM, with a variable MLD and the storage of thermal anomalies beneath the mixed layer, has the essential physics for reproducing the reemergence mechanism.

While the leading pattern of variability is similar in the three panels of Fig. 4, the positive anomaly center in the central Pacific has a southwest to northeast tilt in the AGCM-MLM simulation, but has a nearly zonal orientation in observations and the TOGA-ML simulation. A likely explanation for this difference is the influence of ENSO on North Pacific SST anomalies via the "atmospheric bridge" (Alexander 1992, Lau and Nath 1996) in observations and the TOGA-50m simulations. The SST anomaly in the central North Pacific associated with ENSO is largest at around 35°N, 160°W and extends west towards central Japan and thus projects strongly on the leading pattern of SST variability. Alexander et al. (1999) show that the dominant pattern of temperature anomalies at depth in summer is well correlated (> 0.6) with SST anomalies in the tropical Pacific. Thus, while ENSO is not essential for the reemergence mechanism to occur, it influences the wintertime SST anomalies over the North Pacific that participate in the reemergence process.

We have calculated EEOF 1 in a manner similar to that shown in Fig. 4, but where monthly ocean temperature anomalies at 5 levels: (5, 27.5, 47.5, 65 and 85 m) in the AGCM-MLM simulation are included in the covariance matrix. This analysis indicates how the leading pattern of variability evolves over both time and depth. The surface evolution of the dominant pattern (not shown) is nearly identical to the one for just SST in Fig. 4b. A contour plot of the percent variance

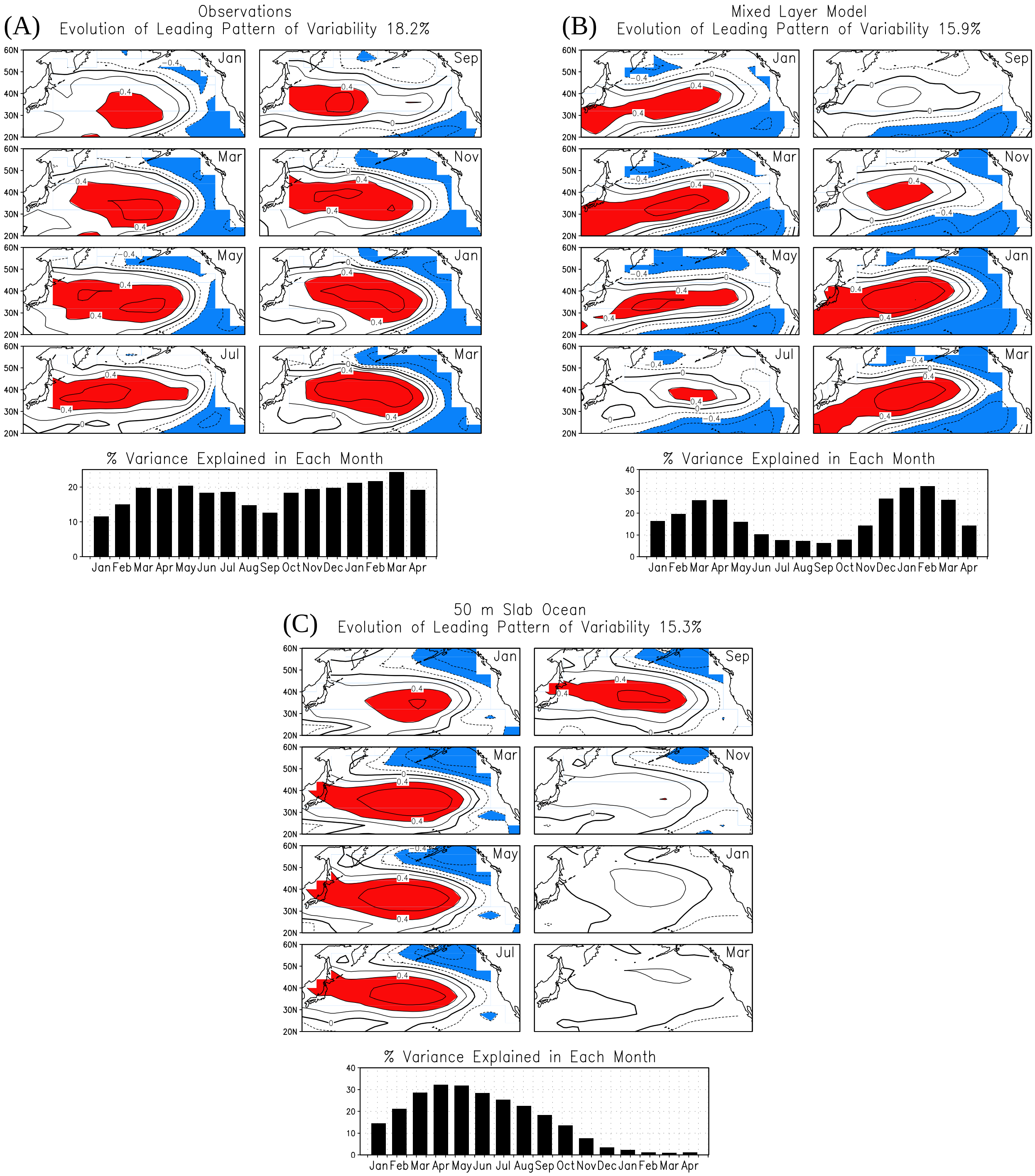

Fig. 4. The leading pattern of SST variability over the seasonal cycle as indicated by EEOF 1 of monthly SST anomalies from January through the following April from 20°N-60°N in the Pacific. The results are presented as the correlation between the time series associated with EEOF 1 with the SST anomalies at the individual grid points for every other month beginning in January (the other months which are not shown indicate a similar evolution). The bottom panel shows the percent variance explained by this EEOF in each month. Results are presented for a) observations derived from the Smith dataset for the years (1950-1999), b) the AGCM-MLM simulation and c) the 4 TOGA-50m simulations. For the latter, EEOF 1 was computed by appending the four 46-year runs to each other, creating a 184-year time series. Contour Interval is 0.2, red (blue) shading for values greater (less) than 0.4 (-0.4).

explained by EEOF 1 in each month from January through the following April for the 5 model levels is shown in Fig. 5. The leading EEOF explains ~23% of the total variance and more than 25% percent of the monthly variance from 0-85 m in the first winter, below 65 m in summer, and from 0-85 m in the subsequent December-March. The leading pattern nearly disappears at the surface in summer, since it encompasses only 4% of the variance in September.

c. Impact of reemergence on SSS and MLD

The limited number of salinity measurements and estimates of mixed layer depth make it impractical to study how anomalies in these fields evolve over the seasonal cycle. Here we examine how the reemergence mechanism influences sea surface salinity (SSS) and MLD in the AGCM-MLM simulation. Correlations between SSS anomailes in FMA and monthly SSS anomalies from the previous January through the following June for each grid square along 52°N are shown in Fig. 6a. Similar to the SST anomalies (see Fig. 3), the SSS autocorrelations drop from high values in the first winter to a minimum in summer and reach a second maximum in the following winter. The SSS correlations tend to be approximately 0.2-0.4 larger than those for SST after July, with the exception of the summer months west of 170ºE. For example, the SSS and SST autocorrelation values in December at 155°W are 0.85 (Fig. 6a) and 0.6 (Fig. 3b), respectively. The higher correlations for SSS are consistent with the findings of Hall and Manabe (1997) who show that SST anomalies are more highly damped by surface fluxes than SSS anomalies, thus the latter would persist longer and have a slower decay of autocorrelation values.

The zonal average across the Pacific at 20°N, 30°N, 40°N, and 50°N of autocorrelations based on SSS anomalies in FMA are shown in Fig. 6b. At 50°N and 40°N, the correlations drop to 0.4 in September and then increase to a maximum of ~0.72 in January and February, respectively. The decrease of SSS correlation in summer is not as strong at 30°N, but the correlation values are similar to the two more northern latitudes during the following winter. At 20°N, the correlations decline through September and are then nearly constant through the following March. The differences in the autocorrelation functions with latitude is likely tied to the seasonal cycle of mixed layer depth since the autocorrelation in precipitation-evaporation, which governs the surface fresh water flux, drops to near zero by June at all latitudes. At 20°N the mean seasonal cycle of MLD is relatively weak and the MLD is about twice as large in summer compared with the other latitudes, allowing SSS anomalies to persist longer through summer but not to rebound as strongly in the following win-

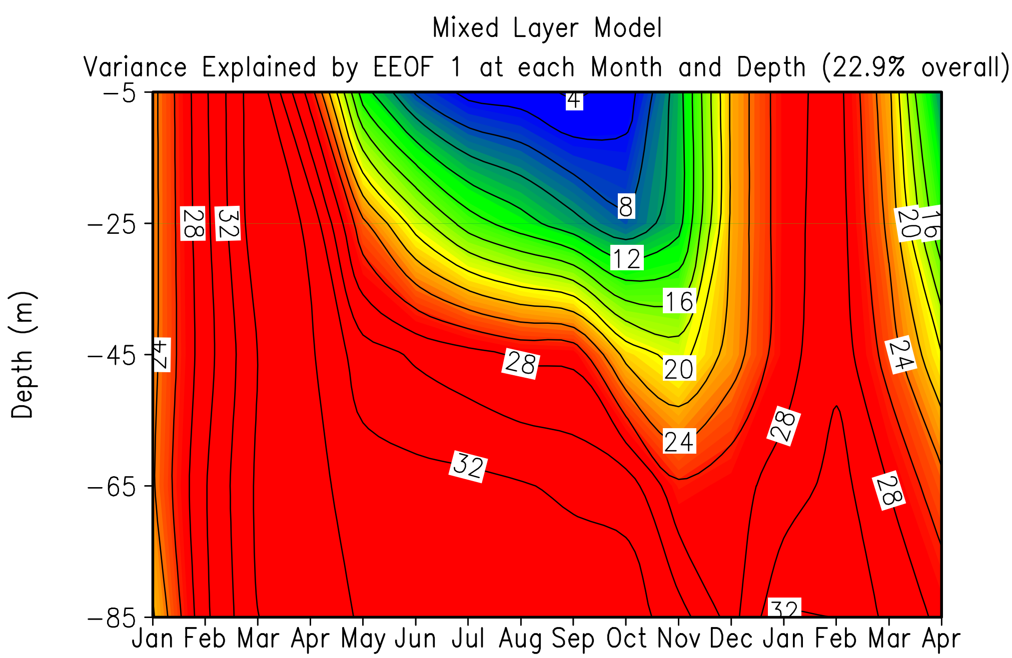

Fig. 5. The percent variance explained by EEOF 1 in the AGCM-MLM simulation when it is computed from ocean temperature anomalies as a function of both month and depth. The horizontal and time domain are the same as in Fig. 3., the five depth level used are 5, 27.5, 47.5, 65 and 85 m. Contour interval is 2%.

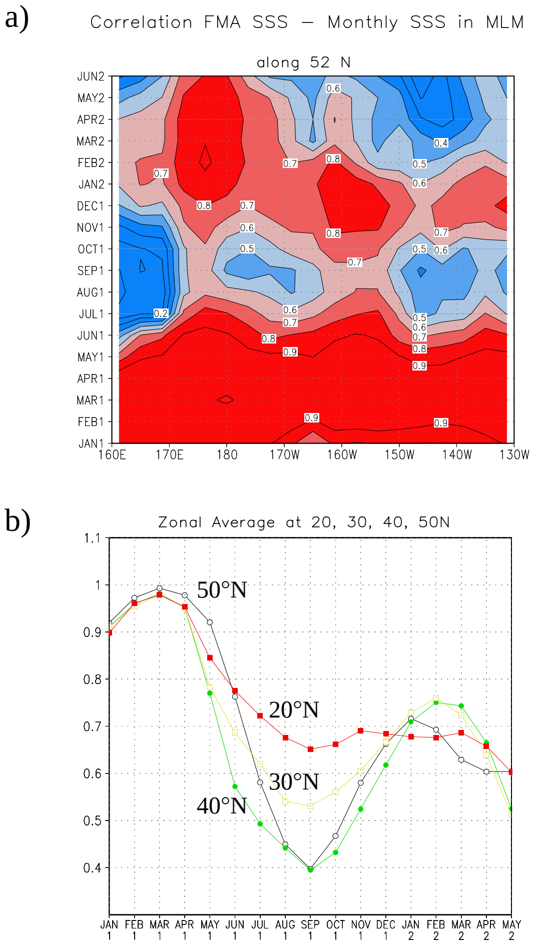

Fig. 6. Lead-lag correlations between SSS anomalies in FMA and monthly SSS anomalies from the previous January through the following June for (a) each grid box along 52°N and (b) zonally averaged across the North Pacific along 20°N, 30°N, 40°N and 50°N from the AGCM-MLM simulation. Contour interval is 0.1.

ter.

Correlations between SST anomalies in FMA and monthly MLD anomalies along 52°N in the MLM are shown in Fig. 7a. Prior to computing the correlations, the MLD anomalies have been smoothed twice using a nine-point smoother, because the spatial extent of the MLD anomalies are much smaller than the SST or SSS anomalies. The SST-MLD correlations are generally negative from January-May, weak but positive (negative) east (west) of 160°W from June-September, and then positive from September-April across the entire basin. The maximum absolute value of the correlations is on the order of 0.4-0.5. The zonal average of the correlations between FMA SST anomalies and the monthly MLD anomalies at 20°,30°,40° and 50°Nare presented in Fig. 7b. Due to the noise in the MLD anomaly fields, there is a fair amount of month-to-month variability in the SST-MLD correlations. Nevertheless, a trend is discernable at all latitudes with negative values in the first January-March that increase through spring and are generally positive though the following winter. The maximum correlations are modest with values of ~0.35 at 30°N and 50°N.

A negative concurrent relationship between SST and MLD has also been documented in the North Pacific by Polovina et al. (1995) and Deser et al. (1996). MLD and SST are anti- correlated since the atmospheric conditions which lead to negative (colder) SST anomalies, enhanced surface cooling through stronger winds and colder drier air, also create positive (deeper) MLD anomalies through convective plumes and mechanical mixing. The reverse is also true. Deser et al (1996) show that the absolute value of negative concurrent SST-

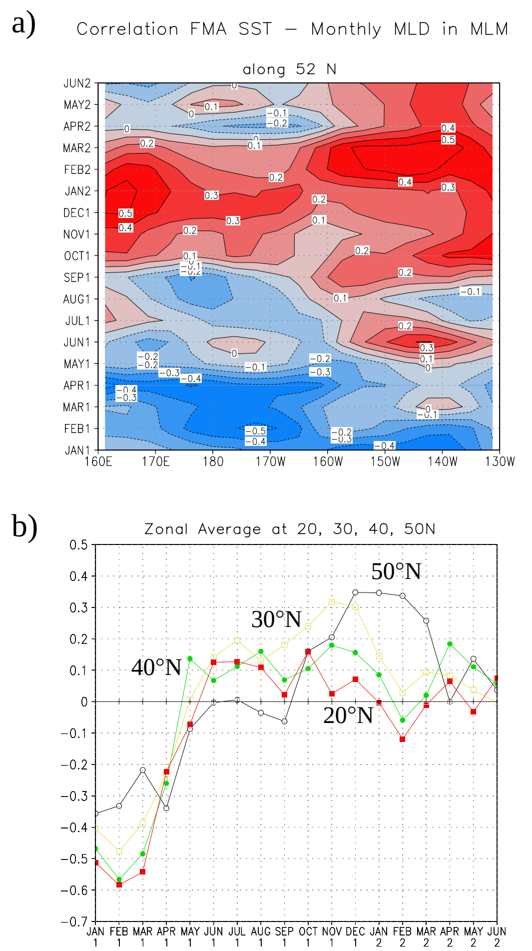

Fig. 7. Lead-lag correlations between SST anomalies in FMA and monthly MLD anomalies from the previous January through the following June for (a) each grid box along 52˚N and (b) zonally averaged across the North Pacific along 20°N, 30°N, 40°N and 50°N from the AGCM-MLM simulation. Contour interval is 0.1.

MLD correlations is greatest in winter, when the MLD is primarily controlled by mixing associated with surface the buoyancy forcing (Alexander et al., 2000). Over most of the North Pacific the temperature decreases with depth, thus enhanced entrainment associated with a deeper mixed layer also tends to cool SSTs. However, Alexander et al. (2000) found that the heat flux anomalies at the base of the mixed layer due to entrainment are small relative to the surface flux anomalies in winter.

The tendency towards positive correlations between winter SSTs and MLD anomalies in the following fall and winter is associated with the mean seasonal cycle of MLD and the reemergence process. When the deep mixed layer in winter shoals, the water left behind affects the density profile in the seasonal thermocline. If the winter mixed layer is warmer (and/or fresher) than normal this would act to reduce the vertical stratification in the seasonal thermocline and thereby increase the penetration depth of the mixed layer for the same amount of surface forcing, especially during the main period of deepening in the following fall and winter. Thus, a positive SST anomaly in winter leads to a positive MLD anomaly in the following seasons, and vice-versa. However, the modest positive correlation values in Fig. 7 and the results of Alexander et al. (2000) indicate that this is a secondary affect compared with the concurrent surface forcing of the mixed layer. We also not that in the MLM the MLD in one winter is not directly related that in the next since the autocorrelation of MLD anomalies decays rapidly and approaches zero by summer.

4. Summary and Discussion

The winter-to-winter recurrence of SST anomalies in the North Pacific have been documented using observed SSTs, subsurface temperature fields from NCEP's ocean data assimilation system, and coupled atmosphere-ocean model simulations. Two types of model simulations are analyzed, in one an AGCM is coupled to a mixed layer ocean model (MLM), while in the second, the same AGCM is coupled to 50 m slab model over the global oceans while observed SSTs are specified as boundary conditions in the tropical Pacific. In the North Pacific, the former simulates a variable depth mixed layer and seasonal thermocline while the latter includes the effects of ENSO but not mixed layer processes. The observations and model simulations performed with the MLM show that temperature anomalies created in the deep winter mixed layer, are strongly damped in the shallow surface layer but stor ed in the seasonal thermocline in summer and then reemerge at the surface in the following winter. However, the model simulations with a 50 m slab ocean simulations did not show evidence for reemergence. The difference between the two indicates that the winter-to-winter recurrence of SST anomalies is due to mixed layer physics and not similar atmospheric forcing in consecutive winters. In addition, while SST anomalies in the tropical Pacific associated with ENSO effect the wintertime SSTs in the North Pacific via changes in the extratropical atmospheric circulation, ENSO events are not essential for reemergence to occur.

Extended EOF analyses indicates that the dominant large-scale SST anomaly pattern that forms in the North Pacific during winter, with anomalies of one sign in the central Pacific ringed by anomalies of the opposite sign, recurs in the following winter as a result of the reemergence mechanism. While this pattern of SST anomalies is driven by the large-scale atmospheric forcing, the reemergence process itself is primarily local in nature, since advection and other horizontal processes are relatively slow in the ocean and do not have sufficient time to change the thermal patterns over the course of a year. In midlatitudes, regions in the eastern, central, and western Pacific all show evidence of the reemergence mechanism, where differences between the three are partly due to geographic variability in the mixed layer depth and the static stability of the upper ocean. The recurrence of both simulated and observed SST anomalies is quite strong in the sub-arctic region of North Pacific, where winter mixed layers are relatively deep. Alexander et al. (2000) found that the effective thermal capacity of the surface layer depends on the MLD in winter, thus in regions of deep mixed layers thermal anomalies are highly persistent from one winter to the next.

In addition to ocean temperatures, the reemergence mechanism also influences salinity and MLD. The autocorrelations of SSS anomalies exceed those of SST, since SST anomalies decay due to negative air-sea feedbacks (upward heat fluxes are enhanced when the water is warmer and vice-versa) while SSS anomalies have a negligible affect on the surface freshwater flux. The reemergence mechanism influences MLD in the following fall and winter through changes in the stratification in the seasonal thermocline. When the winter mixed layer shoals, anomalously cold (warm) water left behind will enhance (reduce) the density jump at the base of the mixed layer and thus retard (enhance) the growth of the MLD in the following fall and winter. However, the reemergence process has only a modest impact on MLD, since the latter is strongly influenced by other processes such as the concurrent surface buoyancy and wind stress forcing.

Through its impact on temperature, salinity and mixed layer depth, the reemergence process could influence biological activity in the upper ocean. For example, changes in MLD in fall as a result of conditions in the previous winter, could alter the amount of time phytoplankton reside in the euphotic zone. In addition, reemergence could affect the primary productivity by changing the phytoplankton biomass or the amount of nutrients available over the seasonal cycle. In some locations, such as western subtropical gyres, a spring bloom near the surface is followed by a relative maximum in phytoplankton within the seasonal thermocline (Doney et al. 1996). Thus, conditions in late winter-early spring within the mixed layer have the potential to influence the amount of nutrients and/or phytoplankton in the seasonal thermocline, and thus the primary productivity at the surface in the subsequent fall and winter when the mixed layer deepens and re-entrains the water below.

Acknowledgements

We thank Thomas Smith, Richard Reynolds, Ants Leetmaa, and Ming Ji at NCEP for providing the ocean temperature analyses. The fields from the TOGA-ML simulations were provided by Gabriel Lau, Isaac Held, and Mary Jo Nath as part of the GFDL-University Consortium Project. This work was supported by NSF grant OCE-9531870 and NOAA grant GC98-139.

References

Alexander, M. A., 1992: Midlatitude atmosphere-ocean interaction during El Niño. Part I: the North Pacific Ocean. *Journal of Climate*, **5**, 944-958.

Alexander, M. A., and C. Deser, 1995: A mechanism for the recurrence of wintertime midlatitude SST anomalies. *Journal of Physical Oceanography*, **25**, 122-137.

Alexander, M. A., C. Deser and M. S. Timlin 1999: The reemergence of SST anomalies in the North Pacific Ocean. *Journal of Climate*, **12**, 2419-2433.

Alexander, M. A. and C. Penland, 1996: Variability in a mixed layer model of the upper ocean driven by stochastic atmospheric surface fluxes. *Journal of Climate*, **9**, 2424-2442.

Alexander, M. A., J. D. Scott, and C. Deser, (2000) Processes that influence sea surface temperature and mixed layer depth in a coupled model. *Journal of Geophysical Research*, accepted.

Barber, R. T. and F. P. Chavez, 1983: Biological consequences of El Niño. *Science*, 222, 1203-1210.

Bathen, K. H. 1972: On the seasonal changes in the depth of the mixed layer in the North Pacific Ocean. *Journal of Geophysical Research*, **77**, 7138-7150.

Beamish , R. J. and D. R. Boullion 1993: Pacific salmon trends in relation to climate. *Can. J. Fish. Aquat Sci.*, **50**, 1002-1016.

Bhatt, U. S., M. A. Alexander, D. S. Battisti, D. D. Houghton and L. M. Keller, 1998: Role of atmosphere-ocean interaction in North Atlantic climate variability. *Journal of Climate*, **11**, 1615-1632.

Brodeur, R. D. and D. M. Ware 1992: Interannual and interdecadal changes in zooplankton biomass in the subarctic Pacific Ocean. *Fisheries Oceanography*, **1**, 32-38.

Cullen, J. J. and M. R. Lewis 1988: The kinetics of algal photoadaptation in the context of vertical mixing. *Journal of Phytoplankton Research*, **10**, 1039-1063.

Delworth, T., 1996: North Atlantic interannual variability in a coupled ocean-atmosphere model. *Journal of Climate*, **9**, 2356-2375.

Denman, K. L. and A. E. Gargett 1995: Bilogical-physical interactions in the upper ocean: the role of vertical and small scale mixing processes. *Annual Review of Fluid Mechanics*, **27**, 225-255.

Derber, J. D. and A. Rosati, 1989: A global oceanic data assimilation system. *Journal of Physical Oceanography*, **19**, 1333-1347.

Deser, C., M. A. Alexander and M. S. Timlin, 1996: Upper ocean thermal variations in the North Pacific during 1970 - 1991. *Journal of Climate*, **9**, 1841-1855.

Deser, C. and M. L. Blackmon, 1995: On the relationship between tropical and north Pacific sea surface temperature variations. *Journal of Climate*, **8**, 1677-1680.

Doney, S. C., D. M. Glover and R. G. Najjar 1996: A new coupled one-dimensional bilogical-physical model for the upper ocean: Applications to JGOFS Bermuda Atlantic timeseries study (BATS) sites. *Deep-Sea Research*, **43**, 591-624.

Ebbesmeyer, C. C., D. R. Cayan, D. R. McClain, F. H. Nichols, D. H. Peterson and K. T. Redmond 1991: 1976 step in the Pacific climate: forty environmental changes between 1968-1975 and 1977-1984. *Proc. of the Proceedings of the Seventh Annual Climate Workshop (PACLIM)*, Asilomar, CA, April, 1990, 115-126.

Elsberry, R. and R. W. Garwood, 1978: Sea surface temperature anomaly generation in relation to atmospheric storms. *Bulletin of the American Meteorological Society*, **59**, 786-789.

Enfield, D. B. and J. S. Allen 1980: On the structure and dynamics of monthly mean sea level anomalies along the Pacific coast of North and South America. *Journal of Physical Oceanography*, **10**, 557-588.

Fasham, M. J. R. 1995: Variations in the seasonal cycle in biological production in subartic oceans: a model sensitivity analysis. *Deep-Sea Research I*, **42**, 1111-1149.

Francis, R. C. and S. R. Hare 1994: Decadal scale regime shifts in the large marine ecosystems of the north-east Pacific: A case for historical science. *Fisheries Oceanography*, **3**, 279-291.

Frankignoul, C., 1985: Sea surface temperature anomalies, planetary waves, and air-sea feedback in the middle latitudes. *Reviews of Geophysics*, **23**, 357-390.

Frankignoul, C. and R. W. Reynolds 1983: Testing a dynamical model for mid-latitude sea surface temperature anomalies. *Journal of Physical Oceanography*, **13**, 1131-1145.

Gaspar, P. 1988: Modeling the seasonal cycle of the upper ocean. *Journal of Physical Oceanography*, **18**, 161-180.

Gill, A. E. and P. P. Niiler 1973: The theory of the seasonal variability in the ocean. *Deep-Sea Research*, 20, 141-177.

Glynn, P. (1990). Global Ecological Consequences of the 1982-83 El Niño-Southern Oscillation. Elsevier, Amsterdam.

Graham, N. E., T. P. Barnett, R. Wilde, M. Ponater and S. Scuhbert, 1994: On the roles of tropical and mid-latitude SSTs in forcing annual to interdecadal variability in the winter Northern Hemisphere circulation. *Journal of Climate*, **7**, 1416-1442.

Hall, A. and S. Manabe, 1997: Can local linear stochastic theory explain sea surface temperature and salinity variability. *Climate Dynamics*, **13**, 167-180.

Ji, M., A. Leetmaa and J. Derber, 1995: An ocean analyses system for seasonal to interannual climate studies. *Mothly Weather Review*, **123**, 460-480.

Jin, F. F., 1997: A theory for interdecadal climate variability of the North Pacific ocean-atmosphere system. *Journal of Climate*, **10**, 1821-1835.

Kalnay, E. and Coauthors, 1996: The NCEP/NCAR 40-year reanalysis project. *Bulletin of the American Meteorological Society*, **77**, 437-471.

Latif, M. and T. P. Barnett, 1994: Causes of decadal climate variability over the North Pacific and North America. *Science*, **266**, 634-637.

Latif, M. and T. P. Barnett, 1996: Decadal climate variability over the North Pacific and North America: dynamics and predictability. *Journal of Climate*, **9**, 2407-2423.

Lau, K. M. and P. H. Chan, 1985: Aspects of the 40-50 day oscillation during the northern winter as inferred from outgoing longwave radiation. *Monthly Weather Review*, **113**, 1889-1909.

Lau, N.-C. and M. J. Nath, 1996: The role of the 'atmospheric bridge' in linking tropical Pacific ENSO events to extratropical SST anomalies. *Journal of Climate*, **9**, 2036-2057.

Mann, K. H. and J. R. N. Lazier 1991: *Dynamics of marine ecosystems, biological-physical interactions in the oceans.* Boston: Blackwell Scientific Publications, 466 pp.

Mantua, N. J., S. R. Hare, Y. Zhang, J. M. Wallace and R. Francis, 1997: A Pacific interdecadal climate oscillation with impacts on salmon production. *Bulletin of the American Meteorological Society*, **78**, 1069-1079.

McFarlane, G. A. and R. J. Beamish 1992: Climatic influence linking Copepod production with strong year-classes in sablefish, Anoplopoma fimbria. *Can. J. Fish Aquat. Sci.*, **49**, 743-753.

Meyers, S. D., M. A. Johnson, M. Liu, J. J. O'Brien and J. L. Spiesberger, 1996: Interdecadal variability in a numerical model of the northeast Pacific Ocean:1970-89. *J. Phys. Oceanogr.*, **26**, 2635-2652.

Mysak, L. A. 1986: El Nino, interannual variability and fisheries in the northeast Pacific Ocean. *Ocean. Can. J. Fish. Aquat. Sci.*, **43**, 464-497.

Nakamura, H., G. Lin and T. Yamagata 1997: Decadal climate variability in the North Pacific in recent decades. *Bulletin of the American Meteorological Society*, **78**, 2215-2226.

Namias, J. and R. M. Born, 1970: Temporal coherence in North Pacific sea-surface temperature patterns. *Journal of Geophysical Research*, **75**, 5952-5955.

Namias, J. and R. M. Born, 1974: Further studies of temporal coherence in North Pacific sea surface temperatures. *Journal of Geophysical Research*, **79**, 797-798.

Pares-Sierra, A. and J. J. O'Brien 1989: The seasonal and interannual variability of the California Current System: a numerical model. *Journal of Geophysical Research*, **94**, 3159-3180.

Philander, S. G. 1990: *El Nino, La Nina, and the Southern Oscillation.* San Diego: Academic Press, Inc. , 293 pp.

Polovina, J. J., G. T. Mitchum and G. T. Evans 1995: Decadal and basin-scale variation in mixed layer depth and the impact on biological production in the Central and North Pacific, 1960-88. *Deep-Sea Research*, **42**, 1701-1716.

Polovina, J. J., G. T. Mitchum, N. E. Graham, M. P. Craig, E. E. DeMartini and E. N. Flint 1994: Physical and biological consequences of a climate event in the central North Pacific. *Fisheries Oceanography*, **3**, 15-21.

Reynolds, R. W. and T. M. Smith 1994: Improved global sea surface temperature analyses using optimum interpolation. J*ournal of Climate*, **7**, 929-948.

Robertson, A. W., 1996: Interdecadal variability over the North Pacific in a multi-century climate simulation. *Climate Dynamics*, **12**, 227-241.

Roemmich, D. and J. McGowan 1995: Climatic warming and the decline of zooplankton in the California Current. *Science*, **267**, 1324-1326.

Sarmiento J. L., R. D. Slater, M. J. R. Fasham, H. W. Ducklow, R. W. Togweiller and G. T. Evans 1993: A seasonal three-dimensional ecosystem model of nitrogen cycling in the North Atlantic euphotic zone. *Global Biogeochemical Cycles*, **7**, 415-450.

Smith, T. M., R. W. Reynolds, R. E. Livezey and D. C. Stokes, 1996: Reconstruction of historical sea surface temperatures using empirical orthogonal functions. *Journal of Climate*, **9**, 1403-1420.

Talley, L. D. 1999: Simple Coupled Midlatitude Climate Models. *Journal of Physical Oceanography*, **29**, 2016-2037.

Tanimoto, Y., N. Iwasaka, K. Hanawa and Y. Toba, 1993: Characteristic variations of sea surface temperature with multiple time scales in the North Pacific. *Journal of Climate*, **6**, 1153-1160.

Trenberth, K. E. and J. W. Hurrell, 1994: Decadal atmosphere-ocean variations in the Pacific. *Climate Dynamics*, **9**, 303-319.

Venrick, E. L., J. A. McGowan, D. A. Cayan and T. L. Hayward 1987: Climate and chlorophyll a: long-term trends in the central North Pacific Ocean. *Science*, **238**, 70-72.

Watanabe, M. and K. M 2000: On the Persistence of Decadal SST Anomalies in the North Atlantic. *Journal of Climate*, submitted.

Weare, B. C. and J. S. Nasstrom, 1982: Examples of extended empirical orthogonal function analyses. *Monthly Weather Review*, **110**, 481-485.

Weare, B. C., A. R. Navato and R. E. Newell, 1976: Empirical orthogonal analysis of Pacific Ocean sea surface temperatures. *Journal of Physical Oceanography*, **6**, 671-678.

White, W. B., 1995: Design of a global observing system for gyre-scale upper ocean temperature variability. *Progress in Oceanography*, **36**, 169-217.

Yukimoto, S., M. Endoh, Y. Kitamura, A. Kitoh, T. Motoi, A. Noda and T. Tokioka, 1996: Interannual and interdecadal variabilities in the Pacific in an MRI coupled GCM. *Climate Dynamics*, **12**, 667-683.

Yoklavich, M. M., V. J. Loeb, M. Nishimoto and B. Daly 1996: Nearshore assemblages of larval rockfishes and their physical environment off Central California during an extended El Niño event, 1991-1993. *Fishery Bulletin.*, **94**, 766-782

Zhang, Y., J. M. Wallace and D. S. Battisti, 1997: ENSO-like interdecadal variability. *Journal of Climate*, **10**, 1004-1020.